Arch. Metall. Mater. **70** (2025), 1, 21-28

DOI: https://doi.org/10.24425/amm.2025.152502

M. SELLAPPAN[1*], V. VASUMATHI[1], V.O. SANGEETHA[2], B. VENKATACHALAPATHY[3], T.M. SRIDHAR[4]

SURFACE MODIFICATION OF 316L SS BY NANO CHITOSAN-YSZ DUPLEX COATINGS FOR DENTAL APPLICATIONS

The development and characterization of nanochitosan-YSZ (Yttria-Stabilized Zirconia) duplex coatings on 316L stainless steel using a dual method for dental applications are the focus of this study. Dental implants have long been integral to restoring oral health, but the high cost of noble material-based implants limits their accessibility to many individuals. As a solution, this research explores the use of innovative materials and techniques to create cost-effective yet biocompatible dental implants. The study involves a dual coating method that combines electrophoretic deposition and dip coating to create a robust and adherent duplex coating. Nanochitosan, a biopolymer, and YSZ, known for its excellent cell adhesion properties, form the basis of the coating material. The characterization of the duplex coatings includes various analytical techniques to assess their physical and chemical properties. This research aims to enhance the long-term stability and functionality of dental implants, making them more affordable and accessible to a wider range of patients, thereby contributing to improved dental health and quality of life.

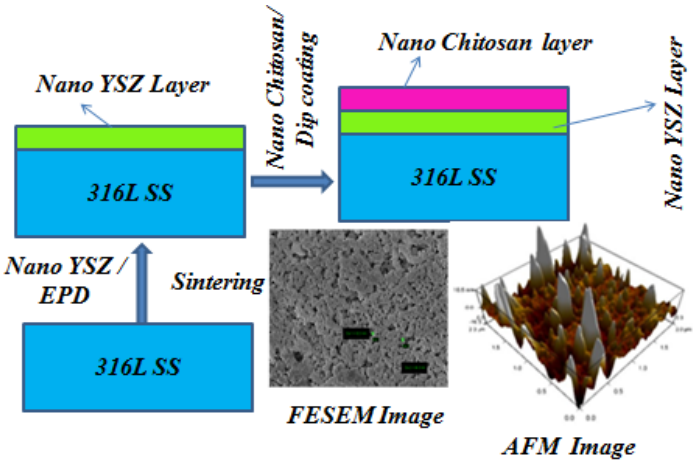

Schematic Representation of the development of nano Chitosan/nano YSZ (Biocomposite) coatings on 316L Stainless steel for dental applications

Keywords: 316L Stainless steel; nano YSZ; EPD; Chitosan; Dip coating

1. Introduction

In the biomedical industry, noble metal-based dental implant materials possess significant effects. Noble material-based dental implants were quite costly, and they are not available for many people at an affordable cost [1]. Dental implants based on alloys such as stainless steel (SS), titanium, and magnesium alloys have been commonly used as a substitute for noble metal-

[1] RAJALAKSHMI ENGINEERING COLLEGE, DEPARTMENT OF CHEMISTRY, CHENNAI - 602105, INDIA
[2] S.A. ENGINEERING COLLEGE, DEPARTMENT OF CHEMISTRY, CHENNAI-600077, INDIA
[3] KARPAGAM ACADEMY OF HIGHER EDUCATION, TAMIL NADU 641021, INDIA
[4] UNIVERSITY OF MADRAS, DEPARTMENT OF ANALYTICAL CHEMISTRY, CHENNAI – 600089, INDIA

* Corresponding author: mohandoss.s@rajalakshmi.edu.in

type dental implants [2]. SS has high demand in developing countries due to its low cost. Stainless steel has been extensively used for orthopedic implants, most effectively because of its availability, affordability, and resistance to corrosion [3]. However, the use of SS as a dental implant has some limitations, as the material corrodes in the oral environment, which may lead to the failure of the dental implant.

The noble dental implants are highly resistant to various ion attacks under different conditions, but the alloys are not highly corrosion-resistant under different conditions [4]. The surface of implant materials gets corroded easily in a low-pH acidic medium due to the release of more ions. Thus, innovative techniques like surface modification of dental implant materials with more corrosion resistance and cell proliferation are the need of the hour. Surface modification with nanobiocomposites possesses high tissue compatibility, high resistance to corrosion, chemical resistance, high toughness, resistance to wear, and high flexural strength. The enhancement of dental impacts is very much affected by the adherence and stability of the substrate coating and coating/bone interfaces.

The stability of the coating influences the mechanical property, and the adhesion influences the physiochemical characteristics of nature. Long-term stability is required when the impact of a physiological medium is considered [5]. Generally, nanobioceramic Yttria stabilized zirconia (YSZ) coated dental implants possess a high chemical inertness character that allows better cell adhesion [6,7], and the addition of biopolymer chitosan increases the values such as good attachment and cell viability, etc. For more than a decade, novel advanced biocomposite coatings based on chitosan and bioinert ceramic yttria stabilized zirconia (nano YSZ) [8] have been developed for dental applications. Chitosan is a well-known biopolymer that has been utilized for several applications due to its properties such as non-toxicity, osteoconductivity, and very good antimicrobial activity.

The coating of chitosan averts the colonization of the bacteria on the stainless steel plate [9]. The advantages of EPD are its simple and cheap power source equipment, which provides highly uniform and crack-free coating from various alcoholic suspensions with controlled deposition rates by varying the applied voltage and coating time. Due to the marked advantages such as ease in obtaining the desired thickness, formation of layers with high purity, stronger adhesion to the substrate, etc., the EPD method was chosen compared to all other methods. The EPD process is considered an effective technique to develop ceramic coatings on functionally graded materials and on complex-shaped substrates [10,11].

It is reported that nano-YSZ-based dental implants showed high mechanical strength and phase stability at various temperatures [12]. Moreover, nano YSZ, along with a biopolymer chitosan-coated dental implant, would be considered an alternative to conventional dental implants as it provides several advantages, such as accelerating the formation of osteoblasts responsible for bone formation. The main advantages of biocomposite chitosan layers are that they are highly resistant to various ion attacks from artificial saliva and that they also accelerate the formation of osteoblasts responsible for bone formation. The mechanical properties and osteogenic properties of the composites can be improved by adding YSZ to chitosan; however, this improves the mechanical strength and osteogenic properties of the composites [13].

To the best of our knowledge, the development of nano-chitosan/YSZ-based coatings for dental applications is rarely reported. In this work, we report nano YSZ coating on 316L stainless steel by EPD, followed by dip coating of nano YSZ coated samples in chitosan solution. Further, the electrochemical behavior of coated samples was evaluated in an artificial saliva medium for dental applications.

The novelty of this study lies in the innovative combination of techniques employed to enhance the properties of 316L stainless steel for dental applications. Firstly, we introduce a nano yttria-stabilized zirconia (YSZ) coating on the stainless steel using an electrophoretic deposition (EPD) process. Subsequently, we employ a dip coating method to further enhance the surface characteristics by immersing the nano YSZ-coated samples in a chitosan solution. This dual-coating approach aims to synergistically leverage the unique properties of both YSZ and chitosan for improved performance. Finally, the electrochemical behavior of these dual-coated samples is systematically evaluated in an artificial saliva medium, providing valuable insights into the potential applications of this novel coating combination in the dental industry.

2. Materials and methods

2.1. Materials

Chitosan (degree of deacetylation 100), Nano YSZ (99.99%) (particle size <100 nm) obtained from Thermo Fischer Scientific The IPA solvents, acetic acid, and other chemicals used were of analytical grade.

2.2. Substrate and suspension preparation

ASTM F-89 standard 316L stainless steel (10×10×2 mm size) samples were used as a working electrode after polishing it mechanically using grit silicon carbide papers, followed by a gentle wash in dilution of HCl and soap oil solution. Further, the samples were ultrasonically cleaned and then dried in an oven. The dried 316L stainless steel substrates were stored in desiccators prior to the EPD process. 2% nano YSZ suspension was prepared by mixing 2 g of nano YSZ powder in isopropyl alcohol. Finally, in order to get an agglomerate-free suspension through the ultrasonication process for about 10 minutes, A 2% chitosan solution was prepared by mixing 2 g of finely ground chitosan flakes in 2% glacial acetic acid. The resultant solution was stirred constantly for 10 hours. The obtained homogeneous solution was stored in a cool place [14].

2.3. Nano YSZ deposition on metal substrate by EPD process and Chitosan coating on nano YSZ surface by Dip coating

316L stainless steel (10×10×2 mm sized) was used as the working electrode, and a thin plate of 314 SS was used as the anode. A distance of about 1cm was maintained between the two electrodes. The working electrode was covered on one side with non-conducting Teflon tape, and then the covered part was dipped in the 2% nanoYSZ suspension so that only the uncovered substrate facing in front of the anode could be coated. During the EPD process, the YSZ suspension was stirred gently. Deposition was carried out on a 1 cm^2 surface area with an applied potential of 70 V at a constant time of 5 minutes. The obtained nano-YSZ coating was gently taken out of the bath and dried at room temperature for 5 minutes, followed by air sintering at 800°C. The structural and morphological properties of the obtained samples were examined.

The chitosan solution was freshly prepared, and nano-YSZ-coated 316L stainless steel samples were dipped completely for 1 to 5 minutes. All the specimens were then gently removed from the chitosan bath. The chitosan-coated samples were dried at room temperature.

2.4. Artificial saliva (AS) preparation

AS was prepared according to the literature reported [15]. Briefly, $C_8H_8O_3$ (2.00g), $C_8H_{16}NaO_8$ (10.00g), KCl (0.625g), $MgCl_2$. $6H_2O$ (0.059g), $CaCl_2.2H_2O$ (0.166g), K_2HPO_4 (0.804 g), and KH_2PO_4 (0.326g) were mixed together in one liter of distilled water. Finally, the pH of AS was adjusted to 6.75 using a KOH solution.

2.5. Characterization

The microstructure and uniformity of nanochitosan/YSZ were investigated using FESEM (Carl Zeis). The Bruker model was used to obtain XRD patterns of nanochitosan/YSZ. An electrochemical workstation (BioLogic SP240) was used to investigate electrochemical impedance spectroscopy. The cell viability of all samples was analyzed by the MTT assay method.

3. Results and discussion

3.1. X-Ray Diffraction Studies (XRD)

The XRD pattern of (a) nano YSZ, (b) chitosan, and (c) nano chitosan/YSZ coatings on 316L stainless steel is represented in Fig. 1. The obtained planes match well with standard JCPDS files No. 82-1246 and 79-0418, confirming the presence of chitosan and nanoYSZ, respectively. The intense peaks appearing at 2θ = 11,19.8, 30.2,50.4, and 60.0 confirm the crystalline nature of nano YSZ and chitosan [17,18] without any impurities in the coatings.

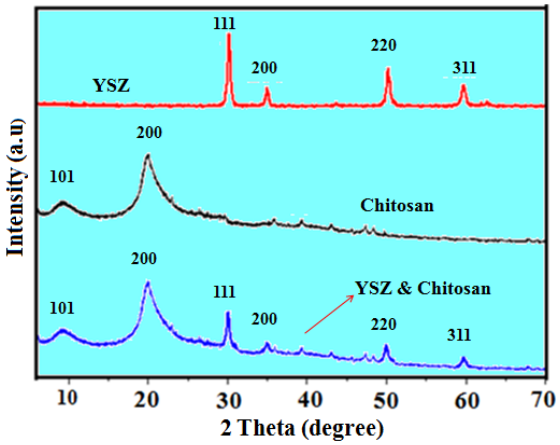

Fig. 1. X-ray diffraction of (a) nano YSZ, (b) Chitosan and (c) nano biocomposite coated on 316L Stainless steel

3.2. Fourier Transform Infrared Spectroscopy (FT-IR)

Fig. 2 represents the FTIR spectra of nano-YSZ and chitosan coated on 316L stainless steel. The peaks at 3500, 2921, 1589, and 1423 cm^1 were accredited to existence of C-H, O-H, N-H, C-O-C and C-N bonds of chitosan respectively [19,20]. The peaks at 636 cm1 indicate the presence of nanoYSZ along with chitosan.

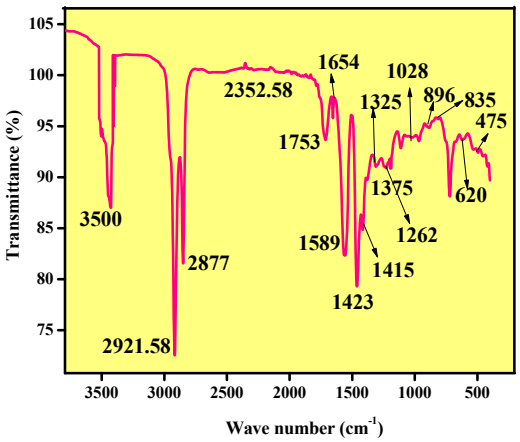

Fig. 2. FTIR spectra of nano biocomposite coated on 316L Stainless steel

3.3. Raman spectroscopy

The phase composition of the coatings was investigated with Raman spectroscopy and depicted in Fig. 3. Four prominent peaks were observed at 256, 322, 466, and 617 cm^1, respectively, conforming to the cubic phase of YSZ. The above peaks are directly associated with the 3Eg, 2B1g, and lA1g symmetries, as predicted for the cubic phase. The prominent peak at 2885 cm^1 corresponds to the m(CH) stretching vibration of the pyranoid ring of chitosan.

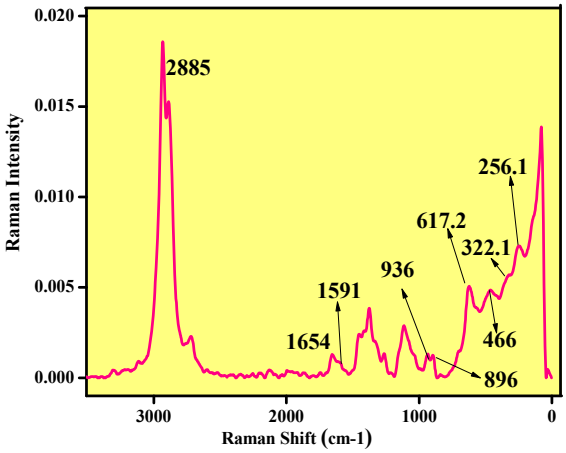

Fig. 3. Raman spectra of nano biocomposite coated on 316L Stainless steel

Thebands at 1654, 1591, 936, and 896 cm^1 are assigned to the ν(CO), $\delta(NH_2)$, ν(CN),) and $\nu(\phi) + \rho(CH_2)$ vibrations ofchitosan,n respectively Therewas as systematic change in band intensity with the change in degree ofdeacetylation,n and the same results were reportedin then literature [21,22]. These results indicate chitosan molecules form thin filmson annano-YSZ-coatedd 316Lstainlesss steel substrate.

3.4. Surface morphological characterization

It is really challenging to obtain a uniform crack-free coating in the EPD process. We have done YSZ coating by the EPD process, and chitosan was coated on the nano-YSZ surface by dip coating. The uniformity and crack nature of the nanochitosan/YSZ biocomposite coating were observed using FESEM. The observed results for the FESEM image of nanochitosan/YSZ are depicted in Fig. 4(a and b). This confirms the uniform, crack-free nature of nanochitosan/YSZ. This study further confirms that the nano YSZ coating was composed of nano grains ranging from 80 to 200 nm and chitosan passivated over nano YSZ nano grains, as shown in FESEM. EDAX analysis was helpful to identify the elemental composition of nanochitosan/YSZ.

The presence of elements such as C, O, Y, Zr, and N in chitosan and nanoYSZ without any impurities. The composition is C = 41%, N = 2%, O = 26%, Y = 5%, and Zr = 26%, as shown in Fig. 5.

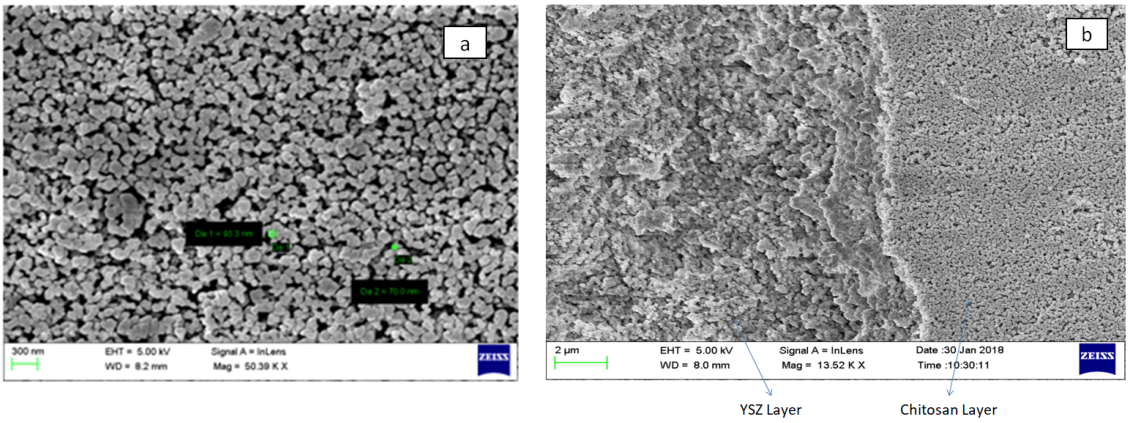

Fig. 4. (a) & (b) FESEM images of nano biocomposite coated on 316L Stainless steel

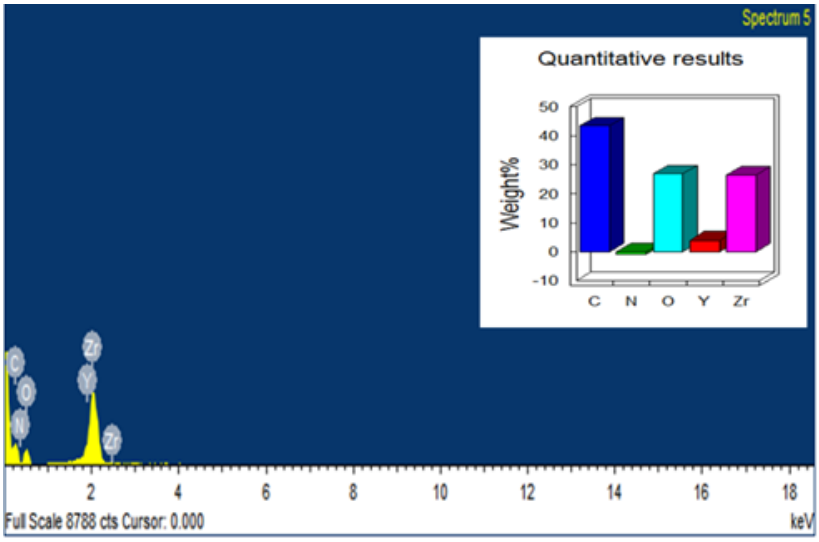

Fig. 5. EDAX spectrum of nano biocomposite coated on 316L Stainless steel

This FESEM and EDAX study further confirms the non-appearance of oxidized products of the base metal (iron oxide) during the sintering process. Further, chitosan and nano-YSZ have not undergone any decomposition during the EPD and dip coating processes.

3.8. Electrochemical studies

3.8.1. Open Circuit Potential (OCP)

As depicted in Fig. 6, a nobler shift was observed for nano YSZ and nano chitosan/YSZ samples compared to uncoated 316L stainless steel samples, indicating better corrosion resistance [24]. It is also noted that the nanochitosan/YSZ coating has the highest nobler shift, which indicates better corrosion resistance when compared to the nanoYSZ coating alone. The OCP time measurement studies confirm that the chitosan layer is highly stable at 1 hour and resists aggressive ion attack from the AS medium when compared to other samples, indicating a better barrier property of the nanochitosan/YSZ coating.

3.8.2. Electrochemical impedance spectroscopy

Electrochemical impedance spectra (EIS) studies were carried out for all the specimens (nano chitosan/YSZ, nano YSZ, and uncoated 316L stainless steel) at OCP after dipping in AS medium (frequency range from 10 kHz to 10 mHz). Fig. 7 represents the EIS and the corresponding equivalent circuit's results. Nanochitosan/YSZ-coated samples show maximum impedance (30 MΩ cm^{-2}) compared to nanoYSZ-coated and uncoated samples. The electrochemical parameters are obtained by Z-Sim curve fitting analysis (TABLE 2).

The chitosan barrier resistance (*Rb*1) and passivation resistance (*Rp*) of nano chitosan/YSZ were maximum when compared to nano YSZ and uncoated 316L stainless steel. The charge transfer resistance of the uncoated specimen is much less than that of nanochitosan/YSZ and nanoYSZ coatings [25]. This indicates that the nanochitosan/YSZ biocomposite layer possesses more resistivity to aggressive ion outbreaks from AS medium. Further, electrons are not transferred from the metal surface to the bulk of the AS medium.

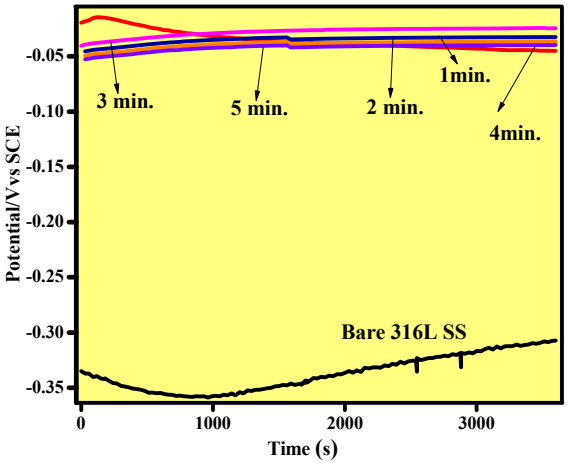

Fig. 6. Open circuit potential time measurement for nano biocomposite coated on 316L Stainless steel in comparison with uncoated 316LSS

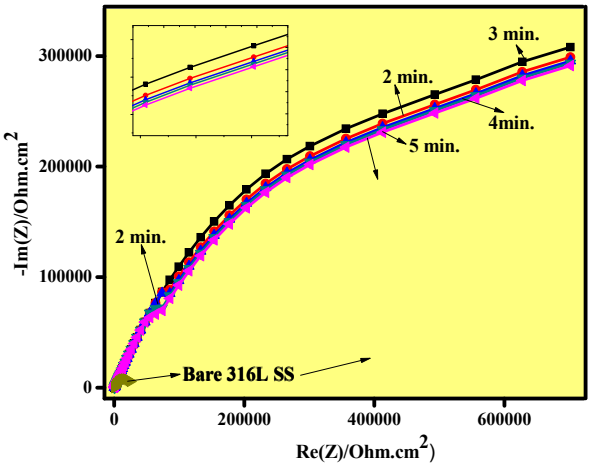

Fig. 7. Nyquist impedance for nano biocomposite coated on 316L Stainless steel in comparison with uncoated 316LSS

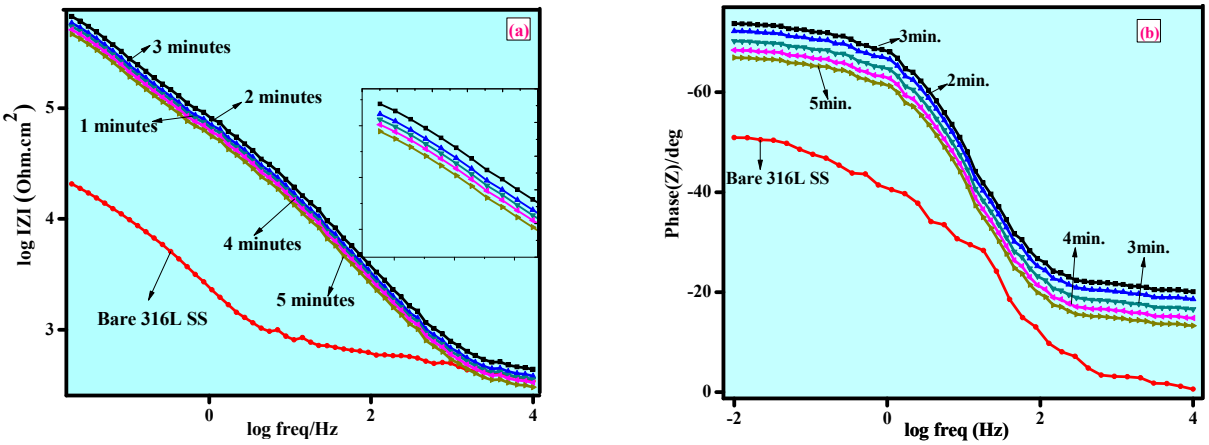

Fig. 8. (a) and (b) Bode impedance and Bode phase for nano biocomposite coated on 316L Stainless steel in comparison with uncoated 316LSS

TABLE 1

Z fit values of nano biocomposite coated (1-5 minutes) 316L Stainless steel samples under AS medium in comparison with uncoated 316L Stainless steel

Biocomposite time intervals	$\|Z\|$ Ω cm^2	RS Ω cm^2	Qcoat (F cm^{-2}sn)	*n*coat	*R*1 (Chitosan layer)	*R*2 YSZ coat	*Qb* (F cm^{-2}sn)	*nb*	*R*3 Ω cm^2	*Cdl* F cm^2	*R*4 Ω cm^2
Bare 316L SS	5644	388	—	0.81	—	—	—	—	190	3.933×10^{-5}	534.5
1 min.	295578	27.8	6.59×10^{-11}	0.31	5.48×10^{6}	1.64×10^{6}	6.89×10^{-10}	0.29	0.98×10^{6}	8.92×10^{-11}	164504
2 min.	299078	24.5	7.49×10^{-11}	0.30	5.76×10^{6}	1.86×10^{6}	7.01×10^{-10}	0.25	1.01×10^{6}	9.04×10^{-11}	168424
3 min.	308078	20.5	8.19×10^{-11}	0.28	5.88×10^{6}	2.06×10^{6}	7.51×10^{-10}	0.22	1.20×10^{6}	9.52×10^{-11}	184484
4 min.	293578	30.8	5.96×10^{-11}	0.33	5.24×10^{6}	1.48×10^{6}	6.64×10^{-10}	0.30	0.86×10^{6}	8.42×10^{-11}	158400
5 min	291278	32.9	5.43×10^{-11}	0.35	5.08×10^{6}	1.24×10^{6}	6.21×10^{-10}	0.31	0.78×10^{6}	8.34×10^{-11}	152444

Fig. 8(a) and (b) represent the bode impedance and bode phase plots. Maximum impedance values were observed for nanochitosan/YSZ. The shape of the phase angle vs. frequency plots indicates the capacitive behavior of the coatings. The phase angle of the nanobiocomposite layer showed a significant shift at −70°, resulting in the nanochitosan/YSZ layer exhibiting highly capacitive behavior when compared to all the other specimens. It was also observed that the corrosion resistivity of nanochitosan/YSZ was significantly higher than that of nanoYSZ-coated and uncoated 316L stainless steel samples.

3.8.3. Cyclic potentiodynamic polarization studies (CPP)

Fig. 9 represents cyclic potential dynamic polarization for nanobiocomposite coated on 316L stainless steel in comparison with uncoated 316L stainless steel. The corrosion current (*Icorr*) and corrosion potential (*Ecorr*) were obtained from the cyclic polarization curves by Tafel fit, and the obtained values are given in TABLE 2 with CPP results. The nanochitosan/YSZ layer possesses a higher corrosion potential of –172.569 mV and a lower corrosion current of 0.001µA compared to other specimens. The *Ecorr* values were shifted in a less negative direction from the uncoated sample to the chitosan-coated sample. The breakdown potential and polarization resistance of nanochitosan/YSZ

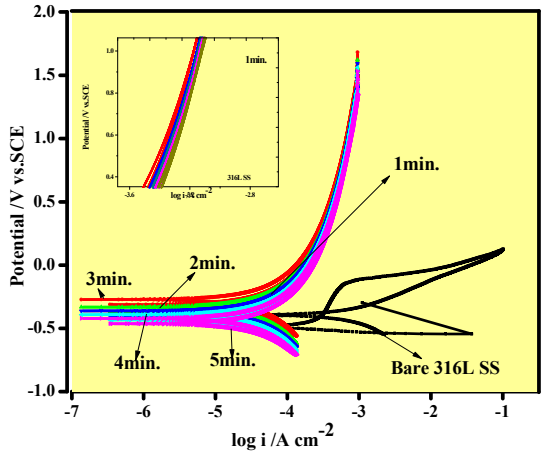

Fig. 9. Cyclic potential dynamic polarisation for nano biocomposite coated on 316L Stainless steel in comparison with uncoated 316L Stainless steel

(1.68211 and 83.3632) were found to be high when compared to nanochitosan/YSZ and uncoated 316L stainless steel due to the nanochitosan/YSZ biocomposite coating. It was not easily destroyed by aggressive ion attack from the AS medium, and this layer resists the release of ions from the substrate to the solution. This result indicates that nano-chitosan/YSZ on the metal surface is more stable and possesses better barrier properties when compared to nano-YSZ and uncoated 316L stainless steel.

TABLE 2

Tafel fit values of nano biocomposite coated (1-5 minutes) samples in AS medium comparison with uncoated 316L Stainless steel

Coating Time	*Ecorr* (mV) vs SCE	*Icorr* µAcm^{-2}	*Rp* (K Ω cm^{-2})
316L Stainless steel	–425	2.308	0.000517
1 min.	–105	0.003	22.03009
2 min.	–98	0.002	34.24105
3 min.	–88	0.001	71.37801
4 min.	–110	0.004	15.54218
5 min	–115	0.005	11.95874

4. Conclusions

Nano YSZ/chitosan uniform crack-free biocomposite coatings were developed on 316L stainless steel by simple, economical EPD and dip coating methods. FESEM and XRD examinations have substantiated the nanometric characteristics of the nanochitosan/YSZ biocomposite, with particles exhibiting a spherical shape. The nanoYSZ particles have an average size ranging from 80 to 200 nm. Analysis of Raman and FTIR spectra has confirmed the successful formation of the nanochitosan/YSZ layer on 316L stainless steel. Electrochemical assessments conducted in artificial saliva have demonstrated that the nanochitosan/YSZ coating displays enhanced corrosion resistance compared to both nanoYSZ and uncoated 316L stainless steel samples. The open-circuit potential (OCP) shifted closer for the biocomposite layer, indicating improved polarization resistance and lower capacitance values, as indicated by electrochemical impedance spectroscopy (EIS) measurements.The nanochitosan/YSZ layer might act as a barrier against attack by corrosive ions and also resist penetration of ions from artificial saliva to metal

surfaces, which was revealed by electrochemical studies. Hence, the optimized biocomposite-coated 316L stainless steel samples would be a new way to fabricate dental implants.

Future work

The present study was aimed to develop bio composite coatings on 316L SS by EPD and dip coating method, so that further invitro cell culture and invivo experimentation with animals have to be carried out to evaluvate the performance of the coated implants. The leaching characteristics of the implants invivo have to be studied and osseointegration process has to be documented in order to pave the way for clinical trials of these coatings.

Acknowledgements

The authors are thankful to the University Grants Commission, India, for their financial support and encouragement (MRP-6134 (SERO/UGC)

REFERENCES

[1] F.H. Schunemann, M.E. Galárraga-Vinueza, R. Magini, M. Fredel, F. Silva, J.C. Souza, Y. Zhang, B. Henriques, Bioactive glass coated zirconia for dental implants: A review. J. Compos. Compd. **98**, 1294-1305 (2019).
DOI: https://doi.org/10.29252/jcc.2.1.2

[2] A. Revathi, A.D. Borrás, A.I. Muñoz, C. Richard, G. Manivasagam, Degradation mechanisms and future challenges of titanium and its alloys for dental implant applications in oral environment. Mater. Sci. Eng. C. **76**, 1354-1368 (2017).
DOI: https://doi.org/10.1016/j.msec.2017.02.159

[3] A. Bekmurzayeva, W.J. Duncanson, H.S. Azevedo, D. Kanayeva, Surface modification of stainless steel for biomedical applications: Revisiting a century-old material. Mater. Sci. Eng. C. **93**, 1073-1089 (2017).
DOI: https://doi.org/10.1016/j.msec.2018.08.049

[4] R.S. Gomes, E.T.P. Bergamo, D. Bordin, A.A.D.B. Cury, The substitution of the implant and abutment for their analogs in mechanical studies: In vitro and in silico analysis. Mater. Sci. Eng. C. **75**, 50-54 (2018).
DOI: https://doi.org/10.1016/j.msec.2017.02.034

[5] Y. Xie, X. Liu, C. Ding, P.K. Chu, Bioconductivity and mechanical properties of plasma-sprayed dicalcium silicate/zirconia composite coating. Mater. Sci. Eng. C. **25** (4), 509-515 (2015).
DOI: https://doi.org/10.1016/j.msec.2005.03.002

[6] L. Wang, X. Liu, G. Wang, W. Tang, S. Li, W. Duan, R. Dou, Partially stabilized zirconia moulds fabricated by stereolithographic additive manufacturing via digital light processing. Mater. Sci. Eng. A. **770**, 138537 (2020).
DOI: https://doi.org/10.1016/j.msea.2019.138537

[7] N.A. Patil, B. Kandasubramanian, Biological and mechanical enhancement of zirconium dioxide for medical applications. Ceram. Int. **46** (4), 4041-4057 (2020).
DOI: https://doi.org/10.1016/j.ceramint.2019.10.220

[8] M. Berni, N. Lopomo, G. Marchiori, A. Gambardella, M. Boi, M. Bianchi, A. Visani, P. Pavan, A. Russo, M. Marcacci, Tribological characterization of zirconia coatings deposited on Ti6Al4V components for orthopedic applications. Mater. Sci. Eng. C. **62**, 643-655 (2016).
DOI: https://doi.org/10.1016/j.msec.2016.02.014

[9] S. Sutha, K. Kavitha, G. Karunakaran, V. Rajendran, In-vitro bioactivity, biocorrosion and antibacterial activity of silicon integrated hydroxyapatite/chitosan composite coating on 316 L stainless steel implants. Mater. Sci. Eng. C. **33** (7), 4046-4054 (2013). DOI: https://doi.org/10.1016/j.msec.2013.05.047

[10] K.P. Ananth, S. Suganya, D. Mangalaraj, J.M.F. Ferreira, A. Balamurugan, Electrophoretic bilayer deposition of zirconia and reinforced bioglass system on Ti6Al4V for implant applications: An in vitro investigation. Mater. Sci. Eng. C. **33** (7), 4160-4166 (2013). DOI: https://doi.org/10.1016/j.msec.2013.06.010

[11] T. Casagrande, G. Lawson, H. Li, J. Wei, A. Adronov, I. Zhitomirsky, Electrodeposition of composite materials containing functionalized carbon nanotubes. Mater. Chem. Phys. **111**, 42-49 (2008). DOI: https://doi.org/10.1016/j.matchemphys.2008.03.010

[12] L. Ruiz, M.J. Readey, Effect of Heat Treatment on Grain Size, Phase Assemblage, and Mechanical Properties of 3 mol% Y-TZP. J. Am. Ceram. Soc. **79** (9), 2331-2340 (1996).
DOI: https://doi.org/10.1111/j.1151-2916.1996.tb08980.x

[13] B. Gaihre, A.C. Jayasuriya, Comparative investigation of porous nano-hydroxyapatite/chitosan, nano-zirconia/chitosan and novel nano-calcium zirconate/chitosan composite scaffolds for their potential applications in bone regeneration. Mater. Sci. Eng. C. **91**, 330-339 (2018).
DOI: https://doi.org/10.1016/j.msec.2018.05.060

[14] X. Geng, O.H. Kwon, J. Jang, Electrospinning of chitosan dissolved in concentrated acetic acid solution. Biomaterials **26** (27), 5427-5432 (2005).
DOI: https://doi.org/10.1016/j.biomaterials.2005.01.066

[15] S.P. Humphrey, R.T. Williamson, A review of saliva: Normal composition, flow, and function. J. Prosthet. Dent. **85** (2), 162-169 (2001). DOI: https://doi.org/10.1067/mpr.2001.113778

[16] J.L. Pozzobon, G.K.R. Pereira,V.F. Wandscher, L.S. Dorneles, L.F. Valandro, Mechanical behavior of yttria-stabilized tetragonal zirconia polycrystalline ceramic after different zirconia surface treatments. Mater. Sci. Eng. C. **77**, 828-835 (2017).
DOI: https://doi.org/10.1016/j.msec.2017.03.299

[17] G. Zhou, P. Jin, Y. Wang, G. Pei, J. Wu, Z. Wang, X-ray diffraction analysis of the yttria stabilized zirconia powder by mechanical alloying and sintering. Ceram. Int. **46** (7), 9691-9697 (2019).
DOI: https://doi.org/10.1016/j.ceramint.2019.12.236

[18] S. Kumari, P.K. Rath, Extraction and Characterization of Chitin and Chitosan from (Labeo rohit) Fish Scales. Procedia Materials Science **6**, 482-489 (2014).
DOI: https://doi.org/10.1016/j.mspro.2014.07.062

[19] J.A.M. Oliveira, R.A.C. de Santana, A.D.O.W. Neto, Characterization of the chitosan-tungsten composite coating obtained by electrophoretic deposition. Prog. Org. Coat. **143** (2020). DOI: https://doi.org/10.1016/j.porgcoat.2020.105631

[20] T. Lertwattanaseri, N. Ichikawa, T. Mizoguchi, Y. Tanaka, S. Chirachanchai, Microwave technique for efficient deacetylation of chitin nanowhiskers to a chitosan nanoscaffold. Carbohydr. Res. **344** (3), 331-335 (2009). DOI: https://doi.org/10.1016/j.carres.2008.10.018

[21] W. Zhu, S. Nakashima, E. Marin, H. Gu, G. Pezzotti, Microscopic mapping of dopant content and its link to the structural and thermal stability of yttria-stabilized zirconia polycrystals. J. Mater. Sci. **55** (2), 524-534 (2020). DOI: https://doi.org/10.1007/s10853-019-04080-9

[22] A. Zając, J. Hanuza, M. Wandas, L. Dymińska, Determination of N-acetylation degree in chitosan using Raman spectroscopy. Spectrochim. Acta A. **134**, 114-120 (2015). DOI: https://doi.org/10.1016/j.saa.2014.06.071

[23] K. GopiSaravanan, M. Bavanilathamuthiah, K.T. Kamalan, Ramachandran, K. Dharini, V. Viswanathan, Y. Vinita, Bio-inspired YSZ coated titanium by EB-PVD for biomedical applications, Surf. Coat. Technol. **307**, 227-235 (2016). DOI: https://doi.org/10.1016/j.surfcoat.2016.08.039

[24] M. Azzi, M. Paquette, J.A. Szpunar, J.E. Klemberg-Sapieha, D.L. Martinu, Tribocorrosion behaviour of DLC-coated 316L stainless steel. Tribol. Int. **42**, 11-12, 1684-1690 (2009). DOI: https://doi.org/10.1016/j.triboint.2009.02.006

[25] Z.H. Jin, H.H. Ge, W.W. Lin, Y.W. Zong, S.J. Liu, J.M. Shi, Corrosion behaviour of 316L stainless steel and anti-corrosion materials in a high acidified chloride solution. Appl. Surf. Sci. **322**, 47-56 (2014). DOI: https://doi.org/10.1016/j.apsusc.2014.09.205